Nanoclay Modification of Shape Memory Polyurethane

J. Dyana Merline[a] and Reghunadhan Nair, C.P.[b]

[a]Department of GRC, The Petroleum Institute, P.O. Box 2533, Abu Dhabi, UAE
[b]Propellants and Special Chemicals Group, PCM Entity, Vikram Sarabhai Space Center, Thiruvananthapuram-695022, India

Abstract

Effect of nanoclay modification on the properties of polytetramethylene oxide-based polyurethane was examined. Nanoclay was dispersed in polyurethane wherein the clay content was varied from 1 to 5 wt.%. The nanocomposites were characterized by thermal, FTIR, XRD and thermo-mechanical analyses and their shape memory properties were evaluated. Morphology was examined by TEM analysis. Bending test was adopted for the evaluation of shape memory property. Increase in clay content resulted an increase in transition temperature. Tensile strength and modulus increased proportional to nanoclay content. The elongation decreased with clay content. Intercalated structure of clay in the PU matrix was observed from XRD studies, which was confirmed by TEM analysis. Modulus ratio showed a decreasing trend with nanoclay content. This resulted in decreased shape recovery characteristics. Highest shape recovery of 92% was observed for PU with 1 wt.% clay content. Moderate nanoclay leveling is conducive to deriving mechanically stronger PU without loss of shape memory characteristics.

Introduction

Although shape memory polymers (SMP) can exhibit unconstrained recoverable strain of the order of 100%, their relative low modulus limits the recoverable stress levels under constraint [1]. Though SMP materials have found application as an actuation material, they have not fully reached their technological potential. A significant draw back of unreinforced SMP materials is their low stiffness compared to metals and ceramics. The low stiffness of SMP resins results in a relatively small recovery force under constraint compared to alternative metal-based active actuation material. A common approach to obtain higher recovery force is to reinforce polymers with stiffer fibers or particulate fillers with filler content often ranging between 10% and 50% by weight [2-7].

To increase the recoverable stress level for structural applications, Gall et al [5] and Liang et al [8] have examined the reinforcements in SMPs in order to enhance the stiffness. Nano-scale reinforcements in polymers can lead to better interface properties than the micro-scale reinforcements and therefore a large increase in modulus and strength [9]. The low density of reinforced or unreinforced SMPs is an advantage for lightweight structural applications. Polyurethanes based on polycaprolactone diol, methylene diisocyanate and 1,4-butane diol and their nanocomposites of reactive nanoclay exhibiting shape memory properties were reported by Cao et al [10]. They studied the variation of shape fixity and shape recovery stress as a function of clay content. Thermoplastic polyurethanes having an alternating sequence of hard and soft segments in which a nanostructured polyhedral oligomeric silsesquioxane diol (POSS) was used as a chain extender to form a crystalline hard segment has been reported [11]. The hybrid polyurethanes exhibited excellent shape recovery effect, which was adjustable according to the composition of the POSS. The developed polyurethanes have multiple applications including, implants for human health care, drug delivery matrices, superabsorbant hydrogels, coatings, adhesives, temperature and moisture sensors, etc.

The roles of graphene in shape memory polyurethane nanocomposite (SMPUN) as reinforcing filler and as a fixed structure for memorizing the original shape by resistive heating were studied by Jin et al. [12]. The hydroxyl groups of graphene enhanced the

* Corresponding author. E-mail: dambrose@pi.ac.ae

reinforcing effect of graphene and its role as a fixed structure due to the improved grafting of polyurethane chains on hydroxyl functionalized graphene during the in situ preparation of SMPUN. Shape memory polymer nanocomposites with properly designed nano-fillers enhances the stiffness and also function as a fixed structures which could be effectively memorize the original shape and consequently minimize the hysteresis [13, 14].

In a previous work, the synthesis and shape memory property of polyurethane (PU) derived from poly (tetramethylene oxide), tolylene diisocyanate and 1,4-butane diol was described [15]. The PU with 85 wt.% hard segment content exhibited ~94% shape recovery. With a view to explore the light weight structural applications, the present work was focused on the modification of this SMP with nanoclay. The effects of clay modification on the properties of the resultant composites are presented in this paper.

Experimental

Materials

Polytetramethylene oxide (PTMO) (Aldrich chemicals, M_n 2000 g/mol), Butane diol (BD, Alfa Biochem) and Tolylene diisocyanate (TDI, Aldrich) were used to synthesize PUs. PTMO and BD were dried in a flash evaporator at 80 °C/3 h before use. AR grade dimethyl formamide (DMF, SRL India) was used as solvent. Claosite® 25A (Southern Clay Products, USA) nanoclay of dimension 13 μ was used as the reinforcement.

Polymer Synthesis

A 500 ml round bottomed, 3 neck RB flask equipped with a mechanical stirrer, nitrogen inlet and a condenser with drying tube was used for the synthesis of PU. N_2 gas was bubbled at 40 °C for 30 min through the dried PTMO (5 g) taken in the flask, to remove traces of absorbed moisture. To this, calculated amount of TDI (10 g) was added drop-wise and the reaction mixture was stirred under N_2 at 65 °C for 2 h to make the isocyanate terminated prepolymer. To this, a dilute solution of BD (10 g) in DMF followed by the remaining quantity of TDI (10 g) was added slowly at 65 °C (total solid-content was kept at 30% in DMF). After mixing completely, the temperature was raised to 85 °C and the reaction was continued for 3 h to get PU solution.

Nanoclay Dispersion

Nanoclay was initially dispersed in DMF by mechanical stirring to get a 30% solution. To the polyurethane solution in DMF, a solution of nanoclay in DMF was added and mechanically stirred for 8 h to get the nanoclay dispersed in the polymer matrix. It was then poured on a glass plate and dried at 65 °C/24 h followed by vacuum drying at 65 °C/24 h to get a thin film. The film drying was ensured by constant weight of the dried film.

Polymer Characterization

Thermal and Spectroscopic Analysis

Thermal studies were performed in a Mettler DSC-20 analyser. The samples (preserved in a dessicator) were heated from – 50 °C to 100 °C at a heating rate of 5 °C/min. DSC data of the first run was used for analysis. IR studies were done in Perkin Elmer GX-A model FTIR spectrophotometer. Spectra were recorded in the range of 4000 to 550 cm^{-1} with a resolution of 4 cm^{-1} using a thin film of the polymer.

X-ray Diffraction Studies

X-ray diffraction studies were performed in a 'X' Pertpro (P Analytical, Netherlands) using the filter Ni, the target as Cu Kα radiation (λ of 1.5405 A°) at 40 Kv and 30 mA current. The diffraction patterns of the samples were recorded with Bragg's angle 2θ from 0 to 40°.

TEM Analysis

The morphology of clay particles in the polymer nanocomposites was determined by TEM analyses. Samples were cut using a Leica Ultracut UCT ultra microtone. Microtomed thin sections were collected on 200 copper mesh grids and examined by a JEOL TEM 2100 electron microscope at 200 Kv in bright field mode.

Mechanical Tests

Mechanical properties were determined with a tensile tester (UTM 4469). The micro tensile test specimens had the dimensions of 75 mm × 5 mm × 1 mm as per ASTM D 412. The gauge length and crosshead speed were 33 mm and 500 mm/min respectively. At least three specimens were tested, and the average of the measured property was taken.

Dynamic Mechanical Analysis

Dynamic mechanical properties were determined in Rheometrics Scientific Model Mark IV (UK) analyzer in the tensile mode at a frequency of 1 Hz. The specimens were heated from –150 °C to 150 °C at a

heating rate of 5 °C/min. The data of storage modulus and tan delta were recorded.

Shape Memory Evaluation

The method of evaluating shape memory alloy was adopted for the polymers [16, 17] as shown in Fig. 1. A straight rectangular strip of polymer of dimension 100 mm × 10 mm × 2 mm was used for the tests. The polymer was heated to a temperature ($T_{trans\ +20\ °C}$) and deformed to an angle (θ_i) (90 °C) and then cooled to ($T_{trans\ -20\ °C}$) fix the deformation. Then the deformed polymer was heated to ($T_{trans\ +20\ °C}$), the change in angle (θ_f) was recorded. The ratio of recovery was found as $(\theta_i-\theta_f)/\theta_i$. The samples were subjected to bending test for five times and the value of fifth attempt was taken.

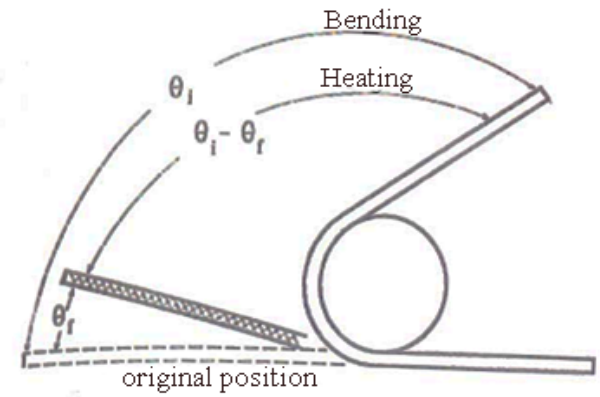

Fig. 1. Schematic representation of bending test.

Results and Discussion

Synthesis and Characterization of PUN

Molar ratio of PTMO: BD: TDI of 1: 45: 46 was chosen for the polyurethane synthesis. The PU consists of 85 wt.% hard segment content which constitutes BD and TDI. The calculations are based on the molecular weight (85 wt.% was calculated by taking the molar ratio of sum of BD and TDI to the total sum of PTMO, BD and TDI). Stoichiometric ratio of OH: NCO was kept as 1:1. Table 1 shows the formulations of nanoclay dispersion in polymer matrix. Nanoclay content was varied from 1 to 5 wt.%. With advancement in wt.% of clay from 1 to 3, drastic change in transition temperature (T_{trans}) (taken from tan delta maxim from DMTA) was observed, but on further increase of nanoclay, only a marginal change in T_{trans} occurs. Compared to the neat PU, (which is also included in Table 1). Polyurethane nanoclay (PUN) systems exhibited comparatively higher transition temperature. This increase in transition was attributed due to the matrix reinforcements by nanoclay that makes the polymer system rigid.

Table 1
Formulations of PUN

Polymer	wt.% of clay	T_{trans} (taken from DMTA)	Shape recovery (%)
PU	0	43	92
PUN-1	1	55	92
PUN-3	3	78	88
PUN-4	4	79	86
PUN-5	5	80	85

Thermal Studies

DSC analysis was performed to study the thermal properties of the nanoclay modified shape memory PU. Figure 2 shows the thermal profiles of PU nanoclay composites. DSC profiles of nanocomposites showed two transitions, one at a lower temperature range of –10 °C to 25 °C and second transition at a higher temperature range of 45 °C to 75 °C. The transition at lower temperature corresponds to melting transition of PTMO segments and the transition at higher temperature corresponds to the glass transition temperature of the polymer system as a whole. With increase in the wt.% of nanoclay, both the transitions shift to higher temperature, which implies the more rigid nature of the nanocomposites with reinforcements. For PUN-4 and PUN-5 with 4 and 5 wt.% of nanoclay, crystal melting is obviously seen at 25 and 20 °C respectively. For the neat PU, crystallization and crystal melting were not clearly observed as shown in Fig. 2.

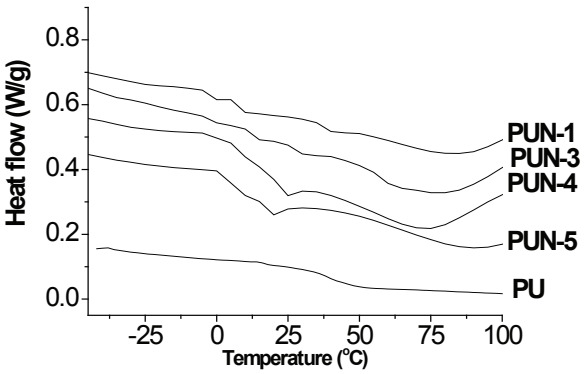

Fig. 2. DSC thermal profiles of PUN.

FTIR Spectroscopic Analysis

FTIR studies were performed on the polyurethane. Figure 3 shows the IR spectra of PUN-1. The FTIR spectra showed presence of –C=O stretching vibration at 1702 cm^{-1}, confirming the presence of urethane linkage. The entire PUN shows similar pattern

in the IR spectra. In a previous study [15], the characteristic –C=O absorption band of unreinforced PU was split into two bands one at 1720 cm^{-1} and another at 1708 cm^{-1} due to the presence of intermolecular hydrogen bonding as shown in Fig. 3. No such splitting was observed in the present study. It is likely that the C=O groups are involved in coordination with the clay components, preventing H-bonding with the urethane NH groups. This reflects in a reduced vibration frequency of the C=O groups (1702 cm^{-1}).

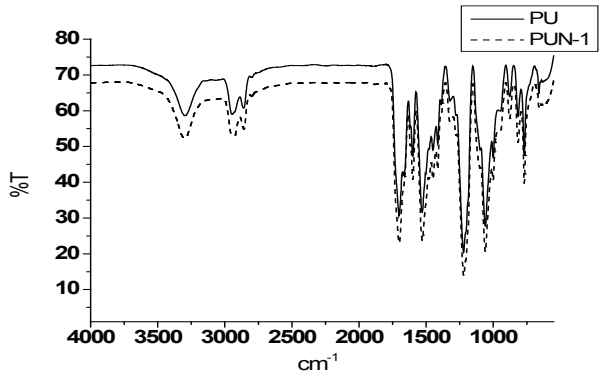

Fig. 3. Comparative FTIR spectra of PUN-1 and PU.

X-ray Diffraction Studies

X-ray diffraction studies were performed to find out the extent of nanoclay dispersion in the polymer matrix. XRD of pure nanoclay is shown in Fig. 4. Diffraction profile exhibited a diffraction maxim at 2θ = 5°, corresponds to d-spacing of 24 A°. XRD pattern of PUNs exhibited diffraction maxima at 2θ = 2.9° confirming the intercalated structure of nanoclay as there occurs a shift in diffraction maxima from 5° to 2.9° in the clay-polymer system as shown in Fig. 5. All the PUN systems exhibited another maximum at 2θ = 4.2°, which implies the existence of layers of clay intercalated to a lesser extent. The absorbance of XRD maxim at 5° confirmed absence of non-intercalated clay components. The intercalated structure was also confirmed by TEM analysis, which will be discussed later.

TEM Analysis

TEM analysis was performed to find out the dispersion of nanoclay in the polymer matrix. Figure 6 shows the TEM pictures of PUN-1 and PUN-5. The intercalated structure of the PUN is clearly seen from the TEM pictures.

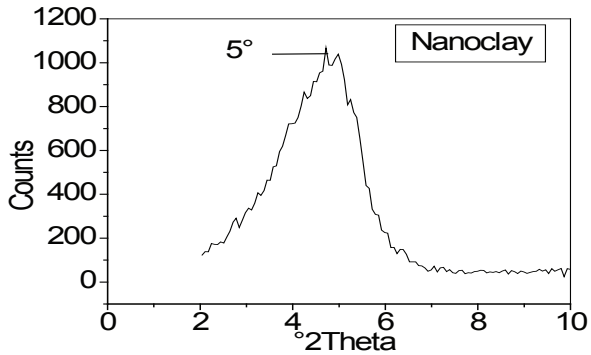

Fig.4 X-ray profile of pure nanoclay.

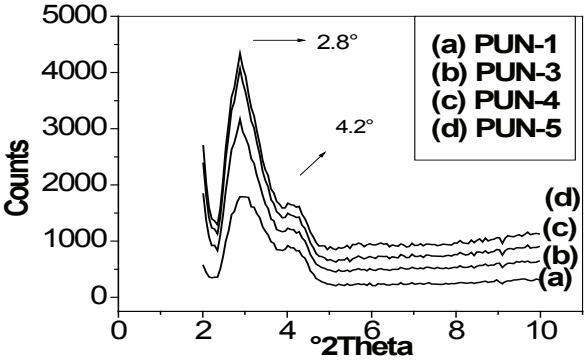

Fig. 5 XRD pattern of PUN.

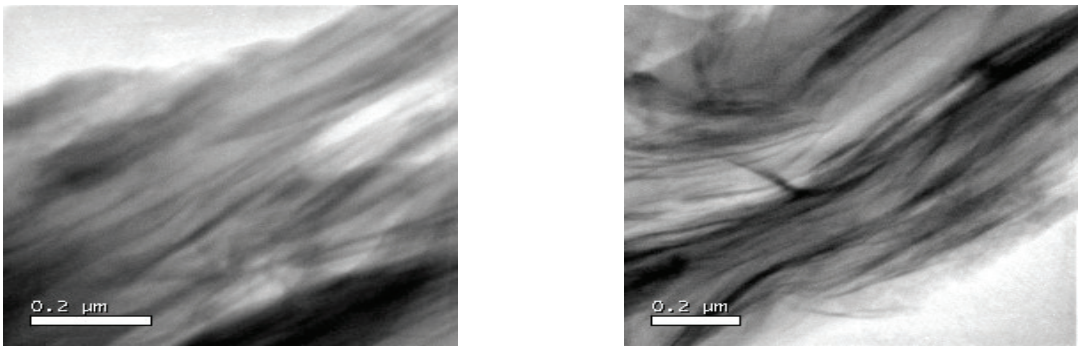

a b

Fig. 6 TEM images of (a) PUN-1 and (b) PUN-5.

Mechanical Properties

Table 2 compiles the mechanical properties of PUN. With advancement in concentration of nanoclay, the elongation decreases and tensile strength increases. At higher nanoclay loading, the intercalation renders the polymer more rigid making it difficult to stretch, accounting for reduced elongation. This is also reflected in the initial modulus. Thus, the mechanical properties of PUN were found to be influenced by nanoclay reinforcements. Compared to the neat polyurethane (PU-85) [15], whose properties are also included in table 2, PUN system exhibited very low % elongation but good mechanical strength. This increase in mechanical properties of nanocomposites is attributed due to the strong interfacial interaction between the matrix and the layered nanocomposites.

Table 2
Mechanical properties of PUN

Sample	Tensile Strength (MPa)	% Elongation	Initial Modulus (MPa)
PU-85 (neat)	4.9 ± 2	300	110 ± 2
PUN-1	21.4 ± 0.2	49.5	400 ± 1.0
PUN-3	23.0 ± 1.0	10	416 ± 7.5
PUN-4	27.2 ± 2.8	9	425 ± 5.0
PUN-5	33.0 ± 1.0	6	650 ± 10

Dynamic Mechanical Thermal Analysis

Figure 7 a,b and c shows the DMA profiles of PUN systems. The DMTA curves show the variation of storage modulus, loss modulus and tan delta. Fig. 7a depicts storage modulus vs temperature curve. Major drop in storage modulus occurs around 20 °C for all the four systems. It is seen that lower nanoclay % leads to higher glassy state modulus. A large glassy state modulus leads to large shape fixity upon cooling and unloading [18]. However comparing modulus ratio which was calculated as $E'_{T_{trans\ +20\ °C}}/E'_{T_{trans\ -20°C}}$, PUN systems exhibited a decreasing trend with nanoclay content. PUN with lowest nanoclay % (1 wt.%) exhibited a modulus ratio of 20. Compared to neat PU discussed in our previous work [12], PUN system exhibited very low modulus ratio. This is because nanoclay reinforces the rubbery state more than the glassy state. This reduction in modulus ratio may possibly be the reason for the diminution in shape recovery characteristics (discussed later). For PUN-1, drop in loss modulus begins at 40 °C, whereas for the other three systems drop in loss modulus begins at 60 °C as shown in Fig. 7 b. With increase in nanoclay content, tan delta peak (Fig. 7 c slightly shifted to high temperature region accounting for increase in the transition temperature. The peak of either loss modulus curve or tan delta curve is often employed to define the transition temperature. Here, we define the polyurethane glass transition as the switching phenomenon. The decrease in modulus due to PTMO moiety is very benign.

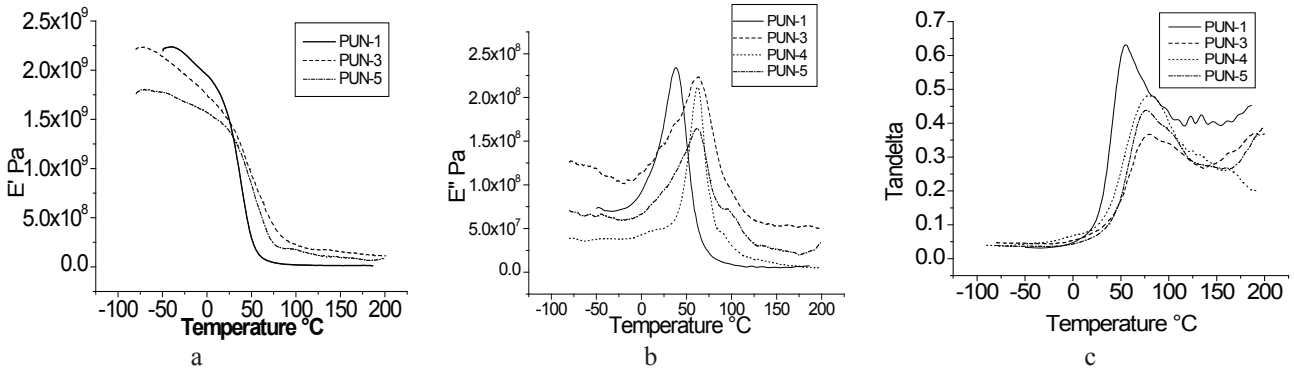

Fig.7. DMTA of PUN (a) Storage modulus vs temperature (b) Loss modulus vs temperature (c) Tandelta vs temperature.

Shape Memory Behavior

Shape memory behavior was done by bending test between the temperatures ($T_{trans\ +20°C}$) and ($T_{trans\ -20°C}$). Table 1 also compiles the shape recovery characteristics of PUN systems. With increase in nanoclay, percentage shape recovery property decreases. This decrease in shape recovery property may possibly due to the effect of nanoclay reinforcements that affects adversely the shape recovery characteristics. Compared to the neat PU, which exhibited 94% shape recovery by bending test, PUN system showed decreased shape recovery property. Maximum shape recovery of 92% was observed for PUN with 1 wt.% clay content. A lowest shape recovery of 85% was observed for PUN with 5 wt.%

of clay content. The poor recovery characteristic is due to the decrease in the modulus ratio as a result of nanoclay reinforcement. Though nanoclay increases the modulus of the PU at above the Tg, the increase in modulus in the post Tg regime is more pronounced. This causes a decrease in the modulus ratio with a consequent penalty in the shape memory properties. This leads to the conclusion that a strong and stiff PU system is realizable at a low nanoclay dispersion with the marginal penalty on shape recovery characteristics

Conclusions

Nanoclay dispersed polyurethane based on PTMO, BD and TDI consisting of 85 wt.% hard segments was prepared by varying the clay content from 1 to 5 wt.%. Increase in clay content resulted an increase in transition temperature. Modulus and tensile strength increased proportional to nanoclay content at the cost of the elongation. XRD studies gave evidence for the presence of intercalated structure of clay in the PU matrix, which was confirmed by TEM analysis. Modulus ratio showed a decreasing trend with nanoclay content. Highest shape recovery of 92% was observed for PUN with 1 wt.% clay content. Nanoclay reinforcement decreases the shape memory property. It is concluded that mechanically sturdy PU systems can be realized that very low nanoclay loading, with marginal penalty on the shape memory properties. Higher clay leading to detrimental for the shape memory properties.

References

1. Y. Liu, K. Gall, M.L. Dunn, P. McCluskey. Mechanics of Mater. 36 (10) (2004) 929-940.
2. K. Gall, M.L. Dunn, Y.P. Liu, D. Finch, M. Lake, N.A. Munshi. Acta Mater. 50 (20) (2002) 5115-5126.
3. H. Tobushi, S. Hayashi, K. Hoshio, N. Miwa. Smart Mater Struct. 15 (2006) 1033-1038.
4. C. Liang, C.A. Rogers, E. Malafeew. J. Intell. Mater. Syst. Struct. 8 (1997) 380-386.
5. K. Gall, M. Mikulas, N.A. Munshi, F. Beavers, M. Tupper. J. Intell. Mater. Syst. Struct. 11 (2000) 877-886.
6. J.W. Cho, S.H. Lee, Eur. Polym. J. 40 (7) (2004) 1343-1348.
7. F.K. Li, L.Y. Qi, J.P. Yang, M. Xu, X.L. Luo, D.Z. Ma. J. Appl. Polym. Sci. 75 (1) (2000) 68-77.
8. C. Liang, C.A. Rogers, E. Malafeew. J. Intel Mater Syst and Struct. 8 (4) (1997) 380-384.
9. S.K. Bhattacharya, R.R. Tummala. J. Electr. Packaging. 124 (1) (2002) 1-6.
10. Q-Q. Ni, C-S. Zhang, Y. Fu, G. Dai, T. Kimura. Composite Structure. 81 (2) (2007) 176-184.
11. T. Ohki, Q-Q. Ni, N. Ohsako, M. Iwamoto. Composites Part: A. Applied Science and Manufacturing 35 (9) (2004) 1065-1073.
12. J.T. Choi, T.D. Dao, K.M. Oh, H. Lee., H.M. Jeong, B.K. Kim. Smart Mater. Struct. 21 (7) (2012) 075017.
13. M.S. Kim, J.K. Jun, H.M. Jeong. Compos. Sci. Technol. 68 (7-8) (2008) 1919-1926.
14. D.H. Jung, H.M. Jeong, B.K. Kim. J. Mater. Chem. 20 (2010) 3458-3466.
15. J.D. Merlline, C.P. Reghunadhan Nair, C. Gouri, G.G. Bandyopadhyay, K.N. Ninan. J. Appl Polym Sci.. 107 (6) (2008) 4082-4092.
16. J.D. Merline, C.P. Reghunadhan Nair, C. Gouri, R. Sadhana, K.N. Ninan. European Polymer Journal 43 (8) (2007) 3629-3637.
17. J.D. Merline, C.P. Reghunadhan Nair, C. Gouri, T. Shrisudha, K.N. Ninan. J. Mater. Sci. 42 (15) (2007) 5897-5902 .
18. B.K. Kim, S.Y. Lee, M. Xu. Polymer 37 (26) (1996) 5781-5799.

Received 12 August 2013